

Atmospheric Corrosion Protection of Epoxy-Coated Stainless Steel by Nanocoating of Decahydrobenzo [8] Annulene-5,10-Disemicarbazone and Tin Filler

Sanojy Misra¹, Rajesh Kumar Singh^{*2}

¹Department of Chemistry, Ranchi University, Ranchi

²Department of Chemistry, Jagdam College, J P University, Chapra, India

Corresponding Author: Rajesh Kumar Singh, Department of Chemistry, Jagdam College, J P University, Chapra, India.

E-mail: rks_jpujc@yahoo.co.in

Citation: Rajesh Kumar Singh et al. (2017), Atmospheric Corrosion Protection of Epoxy-Coated Stainless Steel by Nanocoating of Decahydrobenzo [8] Annulene-5,10-Disemicarbazone and Tin Filler. Int J Nano Med & Eng. 2:4, 17-31.

DOI: 10.25141/2474-8811-2017-4.0017

Copyright: ©2017 Rajesh Kumar Singh et al. This is an open-access article distributed under the terms of the Creative Commons Attribution License, which permits unrestricted use, distribution, and reproduction in any medium, provided the original author and source are credited

Received: February 08, 2017; **Accepted:** April 10, 2017; **Published:** May 02, 2017

Abstract:

Epoxy coating uses for the corrosion protection of stainless steel. It does not protect metal in presence of corrosive pollutants. Epoxycoated stainless steel surface has possessed lots of porosities so pollutants and particulates materials are entered inside by osmosis and diffusion process. Pollutants like oxides of carbon, oxides of nitrogen, and oxides of sulphur form acids and they make hostile environment for base metal and epoxy polymer. These acids develop chemical reaction with epoxy-coated stainless steel. They develop corrosion cell with metal and start corrosion reaction. They can produce several forms corrosion like galvanic, pitting, stress, crevice, blistering and embrittlement. Epoxy polymer is shown swelling corrosion. Such types of pollutants are disintegrated metal and polymer and change their physical, chemical and mechanical properties. Particulates materials are acidic and basic in nature. They are accommodated on the surface of epoxy-coated stainless steel and tarnish their facial appearance. They also produce corroding effects. Weather changes can affect the corrosion rate of materials because increase or decrease temperatures of atmosphere, concentration of pollutants, moisture, humidity and acids. They initiate the corrosion of materials. The corrosion protection of epoxy-coated stainless steel was controlled by the application of synthesized decahydrobenzo [8]annulene-5,10-disemicarbazone and this compound was nanocoated on the surface of epoxy-coated stainless steel. Nanaocoating material develops lot of porosities which are blocked by TiN filler. Nanocoating and filler materials were formed composite a thin barrier on the surface of epoxy-coated stainless steel and studied their action in corrosion in hostile environment. Nanocoating work can be completed by the use of nozzle spray and chemical vapour deposition. Thermal parameters like activation energy, heat of adsorption, free energy, enthalpy and entropy were used to study composite film formation. The corrosion rates of materials were calculated by gravimetric method. Surface coverage areas and coating efficiencies were obtained by the help of corrosion rate. Potentiostat used to determine corrosion potential, corrosion current and current density. Experimental observations indicated that composite film barrier was formed decahydrobenzo[8]annulene-5,10-disemicarbazone and TiN which physical, chemical and mechanical properties did not change easily in ambient environment

Keywords : Hostile Environment, Corrosion, Nanocoating, Filler, Thermal Parameters, Composite Film Barrier

Introduction:

The corrosion of materials is a spontaneously process. It is not fully control but it can be minimized by the application of corrosion protection technique. Epoxy paint is used by automobile industries for corrosion protection. The outer bodies of transport vehicles are made of stainless steel. This metal corrodes in contact of corrosive environment, hence for their protection epoxy-coating is applied on the surface of stainless steel. But this coating cannot

protect stainless steel in H₂O, O₂ (moist), CO₂, NO₂ and SO₂ environment. In these environments for the corrosion protection of epoxy-coated stainless steel was used decahydrobenzo[8]annulene-5,10-disemicarbazone and TiN. The synthesized organic compound decahydrobenzo[8]annulene-5,10-disemicarbazone was nanocoated on the surface of epoxy-coated stainless steel and their porosities were blocked by TiN filler.

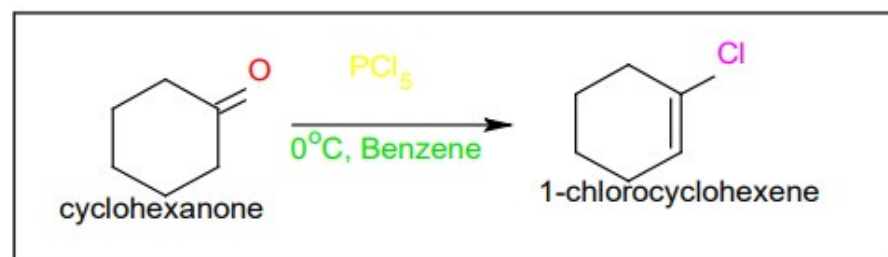
Abrasive blasting is a common method of preparing a metal surface for application of an organic coating (Bhadra S et al

2011). The performance of an organic coating/metal (Szabo T et.al 2011) substrate system in a corrosive environment depends on the nature of the coating, substrate, and interface (Wen N T et.al 2008) between them. The properties of the interfacial region (Boerio F J et.al 2005) are influenced by the abrasive blasting process. The corrosion behavior of coated stainless steel (Deveci H et.al 2012) is significantly affected by the choice of blasting abrasive and the parameters of the blasting process. They investigate the adhesion of polymer coating (Genzer J 2005) systems of the following types: alkyd, acrylic, latex, vinyl, epoxy, coal tar epoxy (LeonSilva U et.al 2010) and a zinc-filled vinyl (Baier RE 2006). For every case zinc-filled vinyl, steel grit abrasive produced the lowest adhesion when compared with based abrasive. The resistance to blistering of both coal tar epoxy and urethane coatings (Liu X Y et.al 2009) on underground steel storage tanks is more severe for tanks blasted with steel grit than for those blasted with silica sand. The effect of abrasive type on the corrosion rate and cathodic delaminating performance of bare and coated pipeline steel. They found a reduction in the corrosion rate in distilled water and delamination rate of an epoxy powder coating (Liao QQ et.al 2009) in Cl⁻ ions solution when the steel was abrasively blasted with alumina (Zhang DQ et.al 2009) compared to steel blasted with steel grit. They interpreted the results in terms of a reduction in catalytic efficiency (Sahoo RR et.al 2009) for the operative cathodic reaction for the alumina-blasted surface, and hypothesized doping of the oxide layer on the steel with aluminum. Cathodic delamination of organic coatings (Raman R et.al 2007) on steel has been widely studied. It is generally believed that the high pH generated by the oxygen reduction reaction at the delaminating front is responsible for the loss of coating adhesion (Li DG et.al 2006). There are several techniques like metallic and nonmetallic coating, inhibitors action, polymeric coating and paint coating (Cristiani P et.al 2008) used to control the corrosion. Metallic coating did not provide good protection in presence of atmospheric pollutants. Polymeric coating (Cristiani P 2005) used in corrosive environment but this coating did not control attack pollutants. They penetrate polymeric barrier and corrode base metal. Its

bonding and bond connective disintegrate in this environment. The nitrogen, oxygen and sulphur containing alkane, alkene, alkyne, aromatic and heterocyclic organic compounds (Videla H et.al 2009) applied as inhibitors against pollutants but they are not protecting materials. These corrosion protection techniques did not shave material by attack of biological micro and macroorganism (Bibber J W 2009). Particulates are also increasing corrosion of materials for their protection (Ghareba GS et.al 2010) above mention methods is used but they do not give suitable results. Effluents and biowastes corrode materials but their protection above mentioned protection techniques used which do not mitigate corrosion. Mixed types of organic inhibitors used which work as anodic and cathodic protection in ambient environment but these inhibitors become passive in aggressive medium. The purpose of this study is to examine composite thin film formation on the surface epoxy-coated stainless steel by nanocoating compound decahydrobenzo[8]annulene-5,10-disemicarbazone and filler TiN.

Methodology

Coupons of epoxy-coated stainless steel kept in corrosive environment and their corrosion rate determined at different temperatures, times and weathers as mentioned 2780K, 2830K, 2880K, 2930K and 2980K temperature and time fixed 24, 48, 72, 96 and 120 hours. Epoxy-coated stainless steel was nanocoated with decahydrobenzo[8]annulene-5,10-disemicarbazone and its corrosion rate calculated at above recorded temperatures and times. TiN filler used on the surface of decahydrobenzo[8]annulene-5,10-diphenylhydrazone and corrosion rate of material determined above mentioned temperatures and times. These results were obtained by the help of weight loss experiment. Potentiostat 173 model EG & PG Princeton used to measured corrosion potential, corrosion current, current density, anodic and cathodic polarization of epoxy-coated



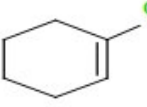
Physical properties of 1-chlorocyclohexene

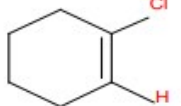
stainless steel, decahydrobenzo[8]annulene-5,10-disemicarbazone epoxy-coated stainless steel and TiN-decahydrobenzo[8]annulene-5,10-diphenylhydrazone epoxy-coated stainless steel. Plasma spray used for nanocoating purpose. The surface adherence properties studied by Arrhenius equation and Langmuir isotherm equation. The composite thin film barrier bonding formation studied by activation energy, heat of adsorption, free energy, enthalpy and entropy. The synthesis process of decahydrobenzo[8]annulene-5,10-

disemicarbazone was given as:

Scheme1: Synthesis of 1-chlorocyclohexene

Cyclohexanone (80g) was added in dry benzene (150ml) and reaction mixture was poured drop wise into a cool solution of PCl5. The mixture was taken in two necks round bottle flask and stirred for further 3hours and during reaction temperature was maintained 0C. The product was extracted from ethereal solution and was washed with 5% aqueous Na2CO3 then after dried with Na2SO4 and solvent removed by application of rotator vapour. The product was purified by column chromatograph by the use of silica gel in petroleum ether. After purification 87% of 1-chlorocyclohexane was obtained.

	Molecular Formula	= C ₆ H ₉ Cl
	Formula Weight	= 116.58866
	Composition	= C(61.81%) H(7.78%) Cl(30.41%)
	Molar Refractivity	= 32.29 ± 0.4 cm ³
	Molar Volume	= 113.5 ± 5.0 cm ³
	Parachor	= 263.4 ± 6.0 cm ³
	Index of Refraction	= 1.480 ± 0.03
	Surface Tension	= 29.0 ± 5.0 dyne/cm
	Density	= 1.02 ± 0.1 g/cm ³
	Dielectric Constant	= Not available
	Polarizability	= 12.80 ± 0.5 10 ⁻²⁴ cm ³
	Monoisotopic Mass	= 116.039278 Da
	Nominal Mass	= 116 Da
	Average Mass	= 116.5887 Da
	M+	= 116.038729 Da
	M-	= 116.039827 Da
	[M+H]⁺	= 117.046554 Da
	[M+H]⁻	= 117.047652 Da
	[M-H]⁺	= 115.030904 Da
	[M-H]⁻	= 115.032002 Da

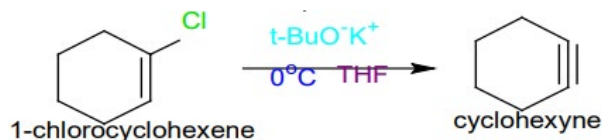
ChemNMR ¹ H Estimation		Estimation quality is indicated by color: good, medium, rough	
	Protocol of the H-1 NMR Prediction (Lib=SU Solvent=DMSO 300 MHz):		
Node	Shift	Base + Inc.	Comment (ppm rel. to TMS)
CH2	1.96	1.96	cyclohexene
CH2	1.99	1.96	cyclohexene
		0.03	generalconnections
CH2	1.74	1.65	cyclohexene
		0.09	generalconnections
CH2	1.61	1.65	cyclohexene
		-0.04	generalconnections
H	5.77	5.59	cyclohexene
		0.18	1-Cl's from 1-ethylene
1H NMR Coupling Constant Prediction			
shift	atom	index	coupling partner, constant and vector
1.96	3	5	7.1 H-CH-CH-H
		8	-1.0 H-CH>C=C>H
1.99	4	8	6.2 H-CH-C (sp2)-H
		6	7.1 H-CH-CH-H
1.74	5	3	7.1 H-CH-CH-H
		6	7.1 H-CH-CH-H
1.61	6	4	7.1 H-CH-CH-H
		5	7.1 H-CH-CH-H
5.77	8	4	6.2 H-C (sp2)-CH-H
		3	-1.0 H>C=C>CH-H

H1NMR of 1-chlorocyclohexene


Scheme2: Synthesis of cyclohexyne

1-Chlorocyclohexene (57g) was dissolved in THF and potassium t-butoxide (BuO-K⁺) was added (75g) at room temperature then after cyclohexene (70ml) was mixed into reaction mixture as trapping agent. After completion of reaction water was poured then it quenched with brine solution and reaction mixture was extracted

from ether. Finally, the compound was dried with sodium sulphate. Solvent was removed by rotator vapour and target product was purified by silica gel column chromatograph. After purification 83% yield of 1,2,3,4,4a,5,6,7,8,8b-decahydrobiphthalene was obtained



Physical properties of cyclohexyne

	Molecular Formula	= C ₆ H ₈
	Formula Weight	= 80.12772
	Composition	= C(89.94%) H(10.06%)
	Molar Refractivity	= 25.79 ± 0.4 cm ³
	Molar Volume	= 91.7 ± 5.0 cm ³
	Parachor	= 217.9 ± 6.0 cm ³
	Index of Refraction	= 1.474 ± 0.03
	Surface Tension	= 31.8 ± 5.0 dyne/cm
	Density	= 0.87 ± 0.1 g/cm ³
	Dielectric Constant	= Not available
	Polarizability	= 10.22 ± 0.5 10 ⁻²⁴ cm ³
	Monoisotopic Mass	= 80.0626 Da
	Nominal Mass	= 80 Da
	Average Mass	= 80.1277 Da
	M+	= 80.062052 Da
M-	= 80.063149 Da	
[M+H] ⁺	= 81.069877 Da	
[M+H] ⁻	= 81.070974 Da	
[M-H] ⁺	= 79.054227 Da	
[M-H] ⁻	= 79.055324 Da	

¹H NMR of cyclohexyne

ChemNMR ¹H Estimation of cyclohexyne

Estimation quality is indicated by color: **good**, **medium**, **rough**

Protocol of the ¹H-NMR Prediction (lb=SU Solvent=DMSO 300 MHz):

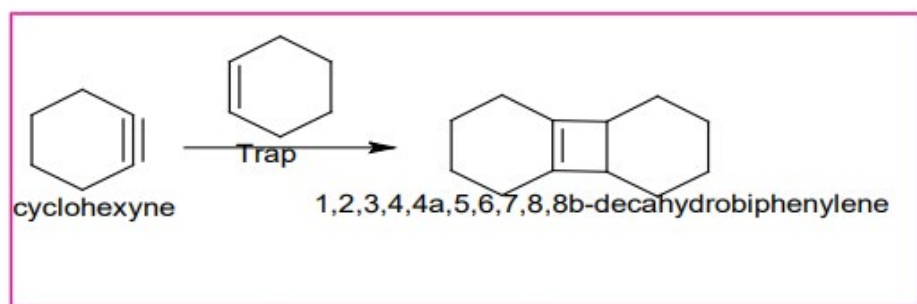
Node	Shift	Base + Inc.	Comment (ppm rel to TMS)
CH2 1.96	1.37	0.65	1 alpha -C+C-C
		-0.06	1 beta -C
		1.37	1 methylene
CH2 1.96	0.65	1.37	1 alpha -C+C-C
		-0.06	1 beta -C
		1.37	1 methylene
CH2 1.44	0.13	1.37	1 beta -C+C-C
		-0.06	1 beta -C
		1.37	1 methylene
CH2 1.44	0.13	1.37	1 beta -C+C-C
		-0.06	1 beta -C
		1.37	1 methylene

¹H NMR Coupling Constant Prediction

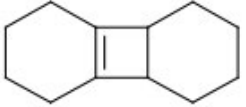
shift	atom	index	coupling partner	constant and vector
1.96	3	5	7.1	H-CH-CH-H
		4	2.5	H-CH-C+C-CH-H
1.96	4	6	7.1	H-CH-CH-H
		3	2.5	H-CH-C+C-CH-H
1.44	5	3	7.1	H-CH-CH-H
		6	7.1	H-CH-CH-H
1.44	6	4	7.1	H-CH-CH-H
		5	7.1	H-CH-CH-H

Scheme3: Synthesis of decahydrobiphenylene

Cyclohexene solution poured into cyclohexyne and reaction mixture was stirred one hours then cyclohexene trapped with cyclohexyne to form an adduct of decahydrobiphenylene.

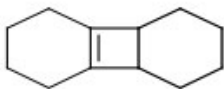


Physical properties of 1, 2,3,4,4a,5,6,7,8,8b-decahydrobiphenylene

	Molecular Formula	= C ₁₂ H ₁₈
	Formula Weight	= 162.27132
	Composition	= C(88.82%) H(11.18%)
	Molar Refractivity	= 50.88 ± 0.4 cm ³
	Molar Volume	= 164.7 ± 5.0 cm ³
	Parachor	= 398.2 ± 6.0 cm ³
	Index of Refraction	= 1.529 ± 0.03
	Surface Tension	= 34.1 ± 5.0 dyne/cm
	Density	= 0.98 ± 0.1 g/cm ³
	Dielectric Constant	= 2.79 ± 0.2
	Polarizability	= 20.17 ± 0.5 10 ⁻²⁴ cm ³
	Monoisotopic Mass	= 162.140851 Da
	Nominal Mass	= 162 Da
	Average Mass	= 162.2713 Da
	M+	= 162.140302 Da
M-	= 162.141399 Da	
[M+H] ⁺	= 163.148127 Da	
[M+H] ⁻	= 163.149224 Da	
[M-H] ⁺	= 161.132477 Da	
[M-H] ⁻	= 161.133574 Da	

H1NMR of 1, 2,3,4,4a,5,6,7,8,8b-decahydrobiphenylene

ChemNMR ¹H Estimation



Estimation quality is indicated by color: **good**, **medium**, **rc**

Protocol of the H-1 NMR Prediction (Lib=SU Solvent=DMSO 300 MHz)

Node	Shift	Base + Inc.	Comment (ppm rel to TMS)
CH	2.15	1.44	cyclohexane
		0.68	1 alpha -C=C from methine
		0.03	1 beta -C=C from methine
CH	2.15	1.44	cyclohexane
		0.68	1 alpha -C=C from methine
		0.03	1 beta -C=C from methine
CH2	1.99,1.890000	1.96	cyclohexene
		-0.02	generalconnections
CH2	1.99,1.890000	1.96	cyclohexene
		-0.02	generalconnections
CH2	1.41,1.310000	1.44	cyclohexane
		0.00	1 beta -C=C from methylene
		-0.08	generalconnections
CH2	1.41,1.310000	1.44	cyclohexane
		0.00	1 beta -C=C from methylene
		-0.08	generalconnections
CH2	1.65	1.65	cyclohexane
CH2	1.65	1.65	cyclohexane
CH2	1.53,1.430000	1.44	cyclohexane
		0.04	generalconnections
CH2	1.53,1.430000	1.44	cyclohexane
		0.04	generalconnections

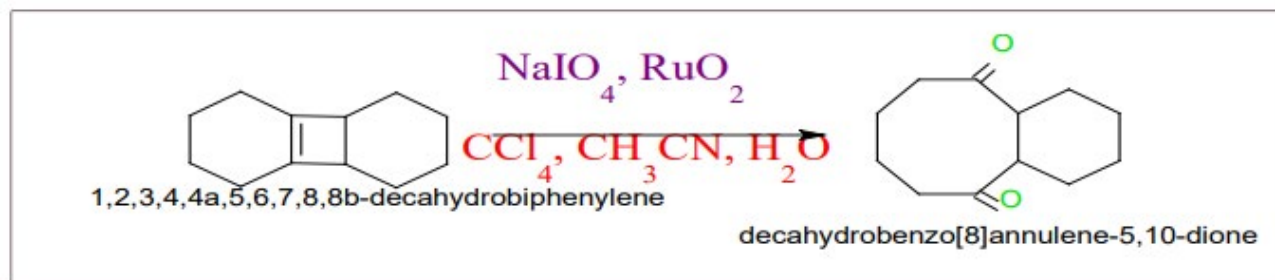
¹H NMR Coupling Constant Prediction

shift	atom	index	coupling partner, constant and vector
2.15	7	8	7.0 H-C-C-H
		9	7.0 H-C-CH-H
2.15	8	7	7.0 H-C-C-H
		12	7.0 H-C-CH-H
1.94	3 diastereotopic	5	7.1 H-CH-CH-H
		6	7.1 H-CH-CH-H
1.94	4 diastereotopic	5	7.1 H-CH-CH-H
		6	7.1 H-CH-CH-H
1.36	9 diastereotopic	7	7.0 H-CH-C-H
		10	7.1 H-CH-CH-H
1.36	12 diastereotopic	8	7.0 H-CH-C-H
		11	7.1 H-CH-CH-H
1.65	5	3	7.1 H-CH-CH-H
		6	7.1 H-CH-CH-H
1.65	6	4	7.1 H-CH-CH-H
		5	7.1 H-CH-CH-H
1.48	10 diastereotopic	9	7.1 H-CH-CH-H
		11	7.1 H-CH-CH-H
1.48	11 diastereotopic	12	7.1 H-CH-CH-H
		10	7.1 H-CH-CH-H

Scheme4: Synthesis of decahydrobenzo[8]annulene-5,10-dione

1,2,3,4,4a,5,6,7,8,8b-decahydrobiphenylene (78g) was taken and was dissolved with carbon tetrachloride. Sodium periodate (NaIO_4) (58g) was added into reaction mixture, then after methylnitrile and water was added. The reaction mixture was stirred 24hours at room temperature. The product was quenched with brine

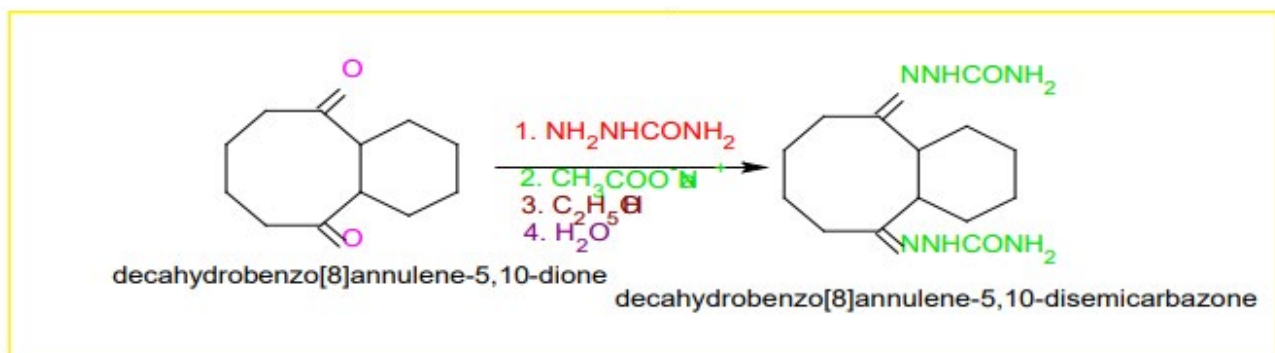
solution then adding sodiumbicarbonate workup was completed with ether and ethereal solution dried with soduimsulphate. The target product was purified by silica gel column chromatograph and 76% yield of decahydrobenzo[8] annulene-5,10-dione was obtained.



Scheme5: Synthesis of decahydrobenzo[8]annulene5,10-disemicarbazone

35g of semicarbazide hydrochloride and 45g of crystallized sodium acetate in 70ml of water was dissolved then 60g of decahydrobenzo[8]annulene-5,10-dione added and shacked. When the mixture was turbid, alcohol or water was added until clear

solution is obtained and again the mixture was shaken for a few minutes and allowed standing. The mixture was warmed on a water bath for 20 minutes and then cooled in ice water. Filtered crystals were washed off with a little cold water and again recrystallized from water or from methanol and got 86% of decahydrobenzo[8] annulene-5,10-disemicarbazone.

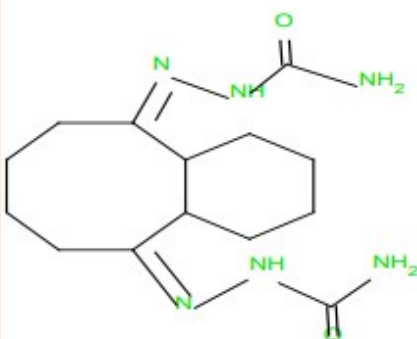


Physical properties of decahydro[8]annulene-5,10-disemicarbazone

	Molecular Formula	= $\text{C}_{14}\text{H}_{25}\text{N}_2\text{O}_2$
	Formula Weight	= 310.39524 ²
	Composition	= C(54.17%) H(8.44%) N(27.08%) O(10.31%)
	Molar Refractivity	= $79.71 \pm 0.5 \text{ cm}^3$
	Molar Volume	= $207.9 \pm 7.0 \text{ cm}^3$
	Parachor	= $590.0 \pm 8.0 \text{ cm}^3$
	Index of Refraction	= 1.692 ± 0.05
	Surface Tension	= $64.7 \pm 7.0 \text{ dyne/cm}$
	Density	= $1.49 \pm 0.1 \text{ g/cm}^3$
	Dielectric Constant	= Not available
	Polarizability	= $31.60 \pm 0.5 \cdot 10^{-24} \text{ cm}^3$
	Monoisotopic Mass	= 310.211724 Da
	Nominal Mass	= 310 Da
	Average Mass	= 310.3952 Da
M+	= 310.211176 Da	
M-	= 310.212273 Da	
[M+H] ⁺	= 311.219001 Da	
[M+H] ⁻	= 311.220098 Da	
[M-H] ⁺	= 309.20335 Da	
[M-H] ⁻	= 309.204448 Da	

H1NMR of decahydro[8]annulene-5,10-disemicarbazone

ChemNMR 1H Estimation



Estimation quality is indicated by color: **good**, **medium**, **rough**

Protocol of the H-1 NMR Prediction (Lib=SU Solvent=DMSO 300 MHz):

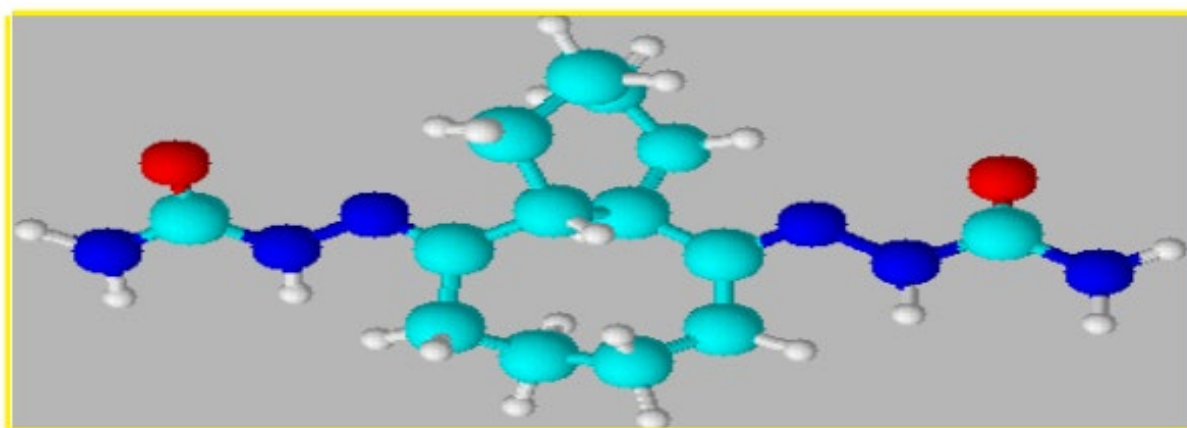
Node	Shift	Base + Inc.	Comment (ppm rel. to TMS)
NH	10.55	7.00	hydrazid
		5.60	1 -C=O from sec am ine
		-2.05	generalconnections
NH	10.55	7.00	hydrazid
		5.60	1 -C=O from sec am ine
		-2.05	generalconnections
NH2	6.21	6.00	usa
		0.21	generalconnections
NH2	6.21	6.00	usa
		0.21	generalconnections
CH	2.26	1.44	cyclohexane
		?	1 unknown alpha substituent(s) from methine
		?	1 unknown beta substituent(s) from methine
		0.82	generalconnections
CH	2.26	1.44	cyclohexane
		?	1 unknown alpha substituent(s) from methine
		?	1 unknown beta substituent(s) from methine
		0.82	generalconnections
CH2	1.74,1.485000	1.44	cyclohexane
		0.25	1 beta -C=N from methylene
		-0.08	generalconnections
CH2	1.74,1.485000	1.44	cyclohexane
		0.25	1 beta -C=N from methylene
		-0.08	generalconnections
CH2	1.53,1.430000	1.44	cyclohexane
		0.04	generalconnections
CH2	1.53,1.430000	1.44	cyclohexane
		0.04	generalconnections
CH2	2.16,2.060000	1.37	methylene
		0.80	1 alpha -C=N
		-0.06	1 beta -C
CH2	2.16,2.060000	1.37	methylene
		0.80	1 alpha -C=N
		-0.06	1 beta -C
CH2	1.58,1.545000	1.37	methylene
		0.25	1 beta -C=N
		-0.06	1 beta -C
CH2	1.58,1.545000	1.37	methylene
		0.25	1 beta -C=N
		-0.06	1 beta -C

1H NMR Coupling Constant Prediction

shift, atom index, coupling partner, constant and vector

shift	atom index	coupling partner	constant	vector
10.55	14			
10.55	19			
6.21	17			
6.21	22			
2.26	7			
		8	7.0	H-C-C-H
		11	7.0	H-C-C-H
2.26	8			
		7	7.0	H-C-C-H
		12	7.0	H-C-C-H
1.61	11 diastereotopic		-12.4	H-C-H
		7	7.0	H-CH-C-H
		9	7.1	H-CH-C-H
1.61	12 diastereotopic		-12.4	H-C-H
		8	7.0	H-CH-C-H
		10	7.1	H-CH-C-H
1.48	9 diastereotopic		-12.4	H-C-H
		11	7.1	H-CH-C-H
		10	7.1	H-CH-C-H
1.48	10 diastereotopic		-12.4	H-C-H
		12	7.1	H-CH-C-H
		9	7.1	H-CH-C-H
2.11	2 diastereotopic		-12.4	H-C-H
		1	7.1	H-CH-C-H
2.11	4 diastereotopic		-12.4	H-C-H
		3	7.1	H-CH-C-H
1.56	1 diastereotopic		-12.4	H-C-H
		2	7.1	H-CH-C-H
		3	7.1	H-CH-C-H
1.56	3 diastereotopic		-12.4	H-C-H
		4	7.1	H-CH-C-H
		1	7.1	H-CH-C-H

XRD of decahydrobenzo[8]annulene-5,10-disemicarbazone

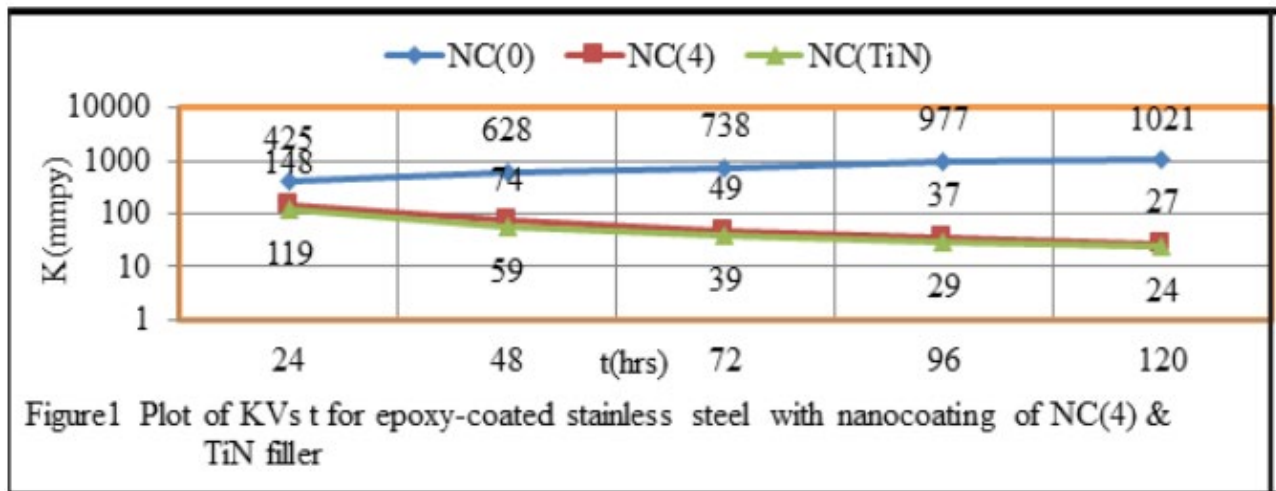


Results and Discussion

The corrosion rate of metal was calculated in the above mentioned environment in absence and presence of nanocoating and filler compounds at 2780K, 2830K, 2880K, 2930K and 2980K temperatures with help of equation $K = 13.56 W/A D t$ (where, W= weight loss of sample in kg, A= surface area of coupon in square meter, D= density in kg M-3, t= exposure time in hour). The corrosion rate of epoxy-coated stainless steel, nanocoating

and filler compounds were obtained at various 24, 48, 72, 96 and 120 hours and their values recorded in table1. Figure1 indicated that corrosion rate of epoxy-coated stainless steel increased absence of coating as time enhanced but these values reduced in presence of nanocoating and filler compounds. They can be improved the quality of surface and minimized corrosion reaction. Nanocoating and filler materials were formed composite thin film barrier i.e. stopped osmosis or diffusion process of pollutants.

NC	Temp(°K)	278°K	283°K	288°K	293°K	298°K	C(mM)
	Times (hrs.)	24	48	72	96	120	
NC(0)	K _o	425	628	738	977	1021	00
	logK _o	2.628	2.797	2.868	2.989	3.001	
NC(4)	K	148	74	49	37	27	50
	logK	2.170	1.869	1.690	1.568	1.431	
	log(K/T)	1.615	1.321	1.149	1.035	0.906	
	θ	0.65	0.88	0.93	0.96	0.97	
	log(θ/1-θ)	0.268	0.865	1.12	1.38	1.509	
	%CE	65	88	93	96	97	
NC(TiN)	K	119	59	39	29	24	20
	logK	2.075	1.771	1.591	1.462	1.380	
	log(K/T)	1.520	1.223	1.051	0.929	0.855	
	θ	0.72	0.91	0.95	0.97	0.98	
	log(θ/1-θ)	0.410	1.004	1.278	1.509	1.690	
	%CE	72	91	95	97	98	



The corrosion of epoxy-coated stainless steel logK versus 1/T in absence and presence of nanocoating and filler compound were plotted in figure 2. Figure 2 reflect that corrosion rate of epoxycoated stainless steel was higher as temperatures rising from 278 to 2980K. But nanocoating of decahydrobenzo[8]annulene-5,10-

disemicarbazone and TiN reduced corrosion rate as temperatures increased. Such types of trends observed clearly in table 1. Both compounds were formed stable barrier which suppressed the corrosion of material.

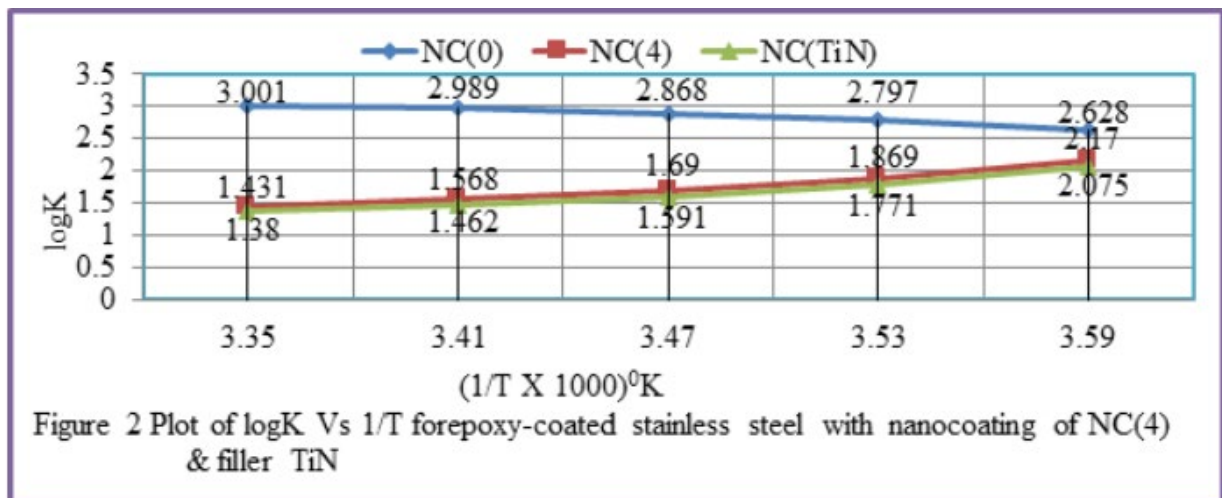


Figure3: plotted between $\log(\theta/1-\theta)$ versus $1/T$ for nanocoated decahydrobenzo[8]annulene-5,10-disemicarbazone and TiN filler. The values of both the compounds $\log(\theta/1-\theta)$ at 278 to 2980K were mentioned in table1. The results of table1 and figure4.5.3 indicate that nanocoating and filler compounds increased the values of $\log(\theta/1-\theta)$ at different temperatures in H₂O, O₂ (moist), CO₂, NO₂ and SO₂ environment.

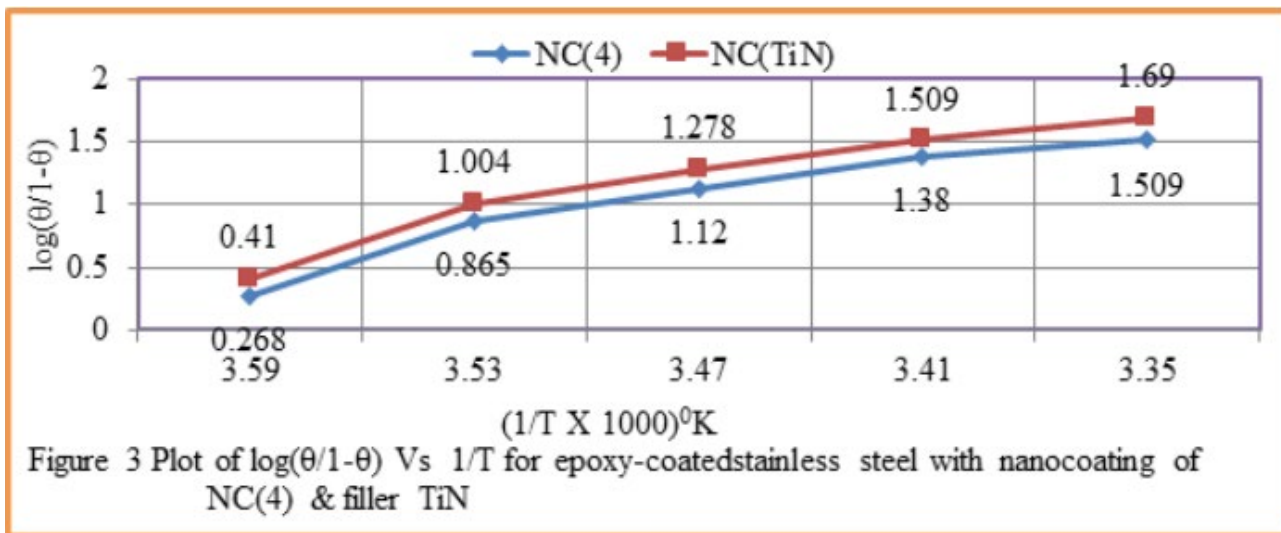


Figure4: plotted between surface coverage area(θ) versus temperature(T) exhibited surface accommodation properties of nanocoating decahydrobenzo[8]annulene-5,10-disemicarbazone and TiN filler. Both compounds enhanced surface coverage area at lower to higher temperature. The surface coverage area at different temperatures calculated by equation $\theta = (1-K/K_0)$ and their values were written in table1. Filler TiN increased more surface coverage area which blocked the porosities of nanocoating compound.

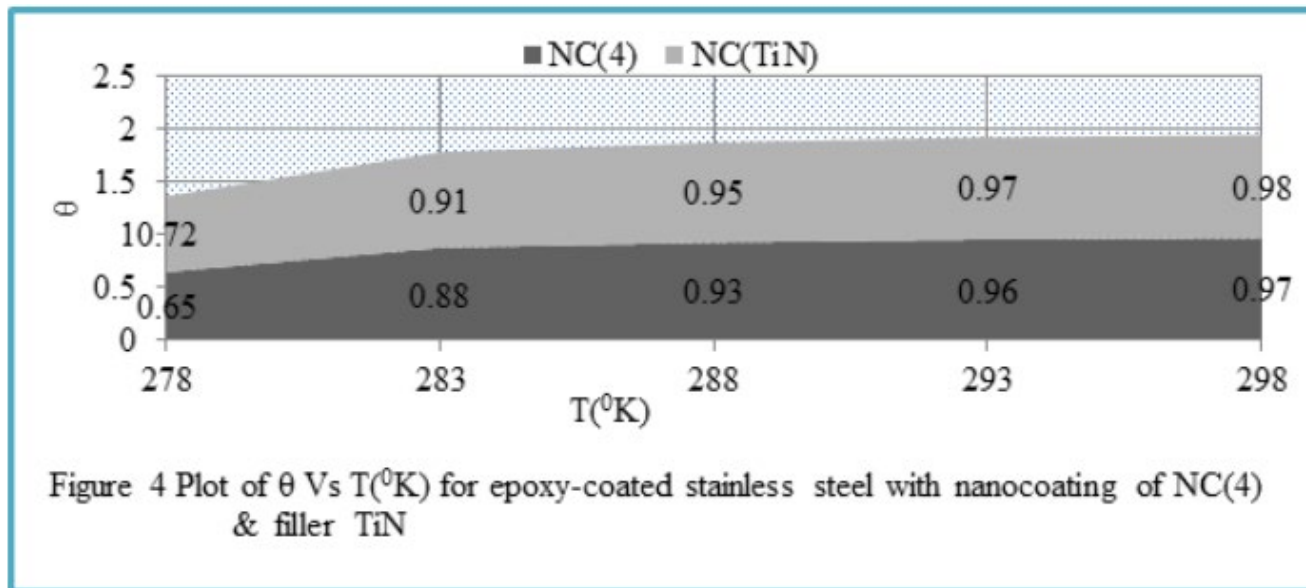


Figure.5: plotted between percentages coating efficiency (%CE) versus temperature (T) at different temperatures for nanocoating and filler compounds. The nature of graph show that nanocoating decahydrobenzo[8]annulene-5,10-disemicarbazone and TiN filler rising % coating efficiency at different temperatures. The % coating efficiency at different intervals of temperatures were calculated by equation $\%CE = (1-K/K_0) \times 100$ and their values were mentioned in table1.

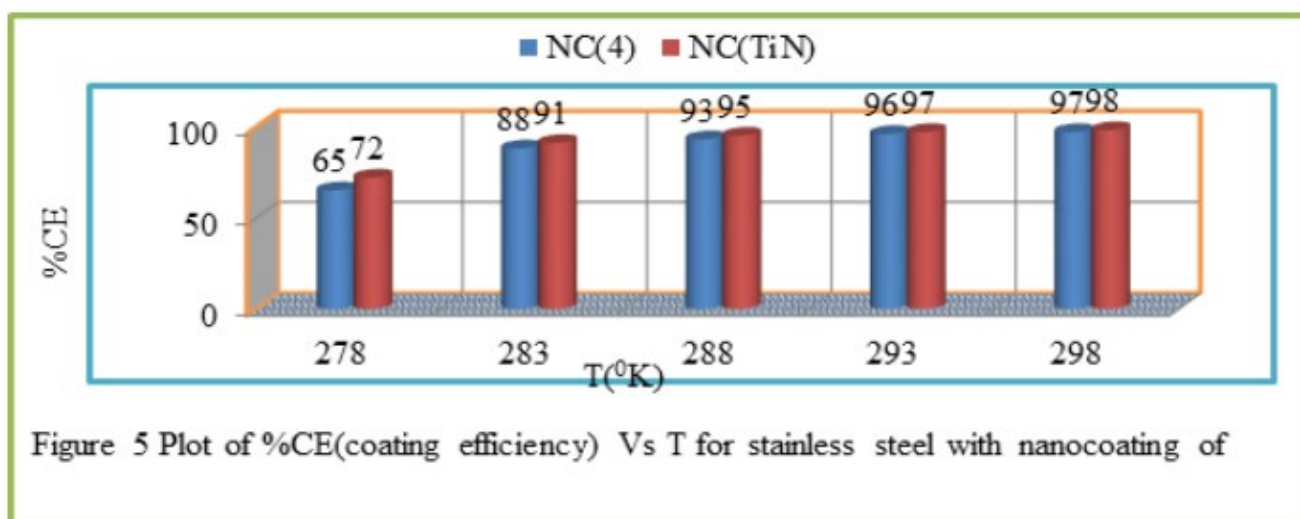


Figure2 is a straight line Arrhenius plot between $\log K$ versus $1/T$ with help of this figure and Arrhenius equation $d/dT(\ln K) = A e^{-E_a/RT}$ were calculated activation energy of epoxycoated stainless steel and nanocoating of decahydrobenzo[8] annulene-5,10-disemicarbazone and TiN filler and their values were written in table4.5.2. In all case activation energy found to be positive sign. It was observed that without coating activation energy increased but their values reduced after nanocoating and filler compounds. Both compounds occupied on the surface of epoxy-coated stainless steel by chemical bonding.

Figure3 indicated straight line plot between $\log(\theta/1-\theta)$ versus $1/T$ for nanocoating of decahydrobenzo[8] annulene-5,10-disemicarbazone and TiN filler and it is a plot of Langmuir isotherm. Heat of adsorption of both nanocoating and filler compounds were determined by equation $\log(\theta/1-\theta) = \log(AC) - (q/2.303 R T)$ and figure3. The values of heat of adsorption are mentioned in table2. Both compounds produced negative sign of energy which confirmed that nanocoating and filler compound formed thin film on the surface of epoxy-coated stainless steel by chemical bonding. Free energy of nanocoating of decahydrobenzo[8] annulene-5,10-

disemicarbazone and TiN filler were calculated by equation $-\Delta G = 2.303 \log R T$ and their results were expressed in table2. The negative values of free energy express that nanocating and filler compounds were adhered with base material by chemical bonding. Free energy results show that coating is an exothermic process. Enthalpy and entropy of nanocoating of decahydrobenzo[8] annulene-5,10-disemicarbazone and TiN filler were calculated by transition state equation $K = R T / N h \log (\Delta S^\ddagger / R) \times \log (-\Delta H^\ddagger / R T)$ and figure6 and their values are recorded in table2. These thermal parameters indicated that nanocoating and filler compounds were attached with base material by chemical bonding. Entropy of both the compounds show that nanocoating and filler compounds arranged on the surface of base material in ordered matrix. Thermal values of activation energy, heat of adsorption, free energy, enthalpy and entropy were confirmed that decahydrobenzo[8]annulene-5,10-disemicarbazone and TiN filler were adhered with epoxy-coated stainless steel by chemical bonding. These thermal parameters also noticed that nanocoating and filler compounds formed passive barrier which stable in higher temperature and corrosive medium.

Table.2: Thermal parameters of nanocoating decahydrobenzo[8]annulene-5,10-disemicarbazone and TiN filler for epoxycoated stainless steel

Thermal parameters	278°K	283°K	288°K	293°K	298°K
NC(0)Ea	180	191	192	197	195
NC(4) Ea	160	137	122	112	105
NC(4)q	-10.03	-52.74	-70.96	-87.86	-95.42
NC(4)?G	-258	-234	-218	-205	-194
NC(4)?H	-116	-95	-81	-71	-63
NC(4)?S	-104	-93	-86	-81	-77
θ NC(4)	0.65	0.88	0.93	0.96	0.97
NC(TiN)Ea	159	135	121	111	103
NC(TiN)q	-24.79	-63.27	-79.45	-93.21	-101.38
NC(TiN)?G	-249	-225	-210	-201	-188
NC(TiN)?H	-107	-85	-73	-65	-57
NC(TiN)?S	-99	-88	-82	-78	-73
θ NC(TiN)	0.72	0.91	0.95	0.97	0.98

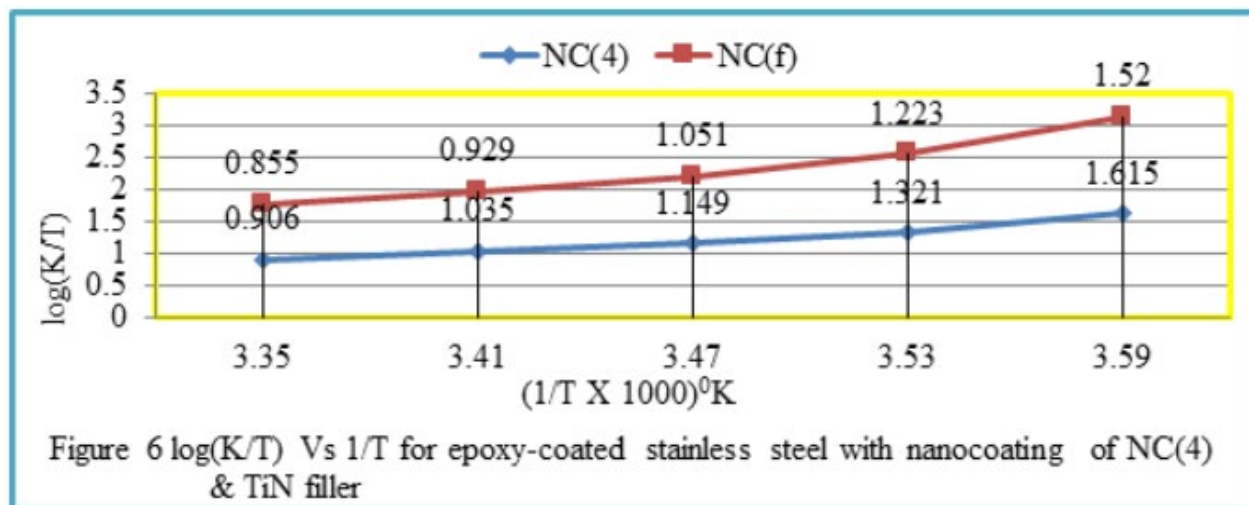


Figure.7: draws graph between enthalpy (ΔE), entropy (ΔS) and surface coverage area (θ) versus temperatures (T) for decahydrobenzo[8] annulene-5,10-disemicarbazone and TiN in H₂O, O₂ (moist), CO₂ and SO₂ environment. The nature of plot indicate that the values of enthalpy and entropy decreased as temperatures rise which enhanced surface coverage area such results trend were observed in table.2.

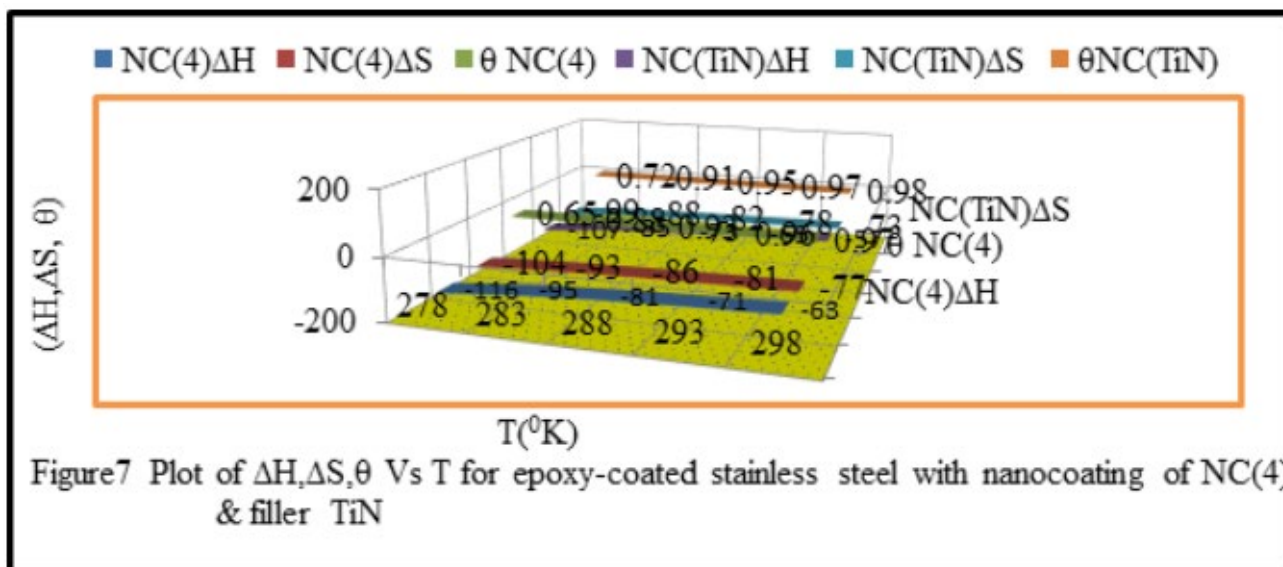
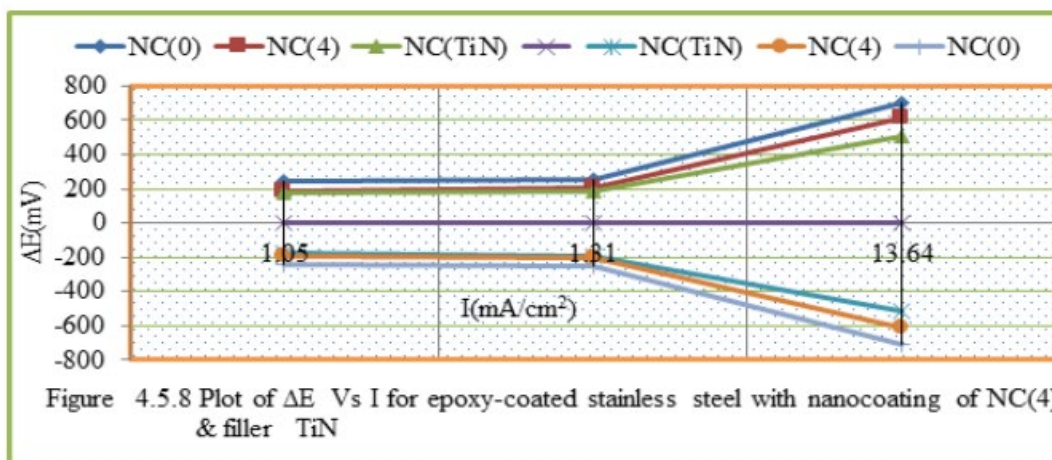


Figure8 was a Tafel plot which was drawn between electrode potential (ΔE) versus current density (I) for nanocoating decahydrobenzo[8] annulene-5,10-disemicarbazone and TiN filler. The corrosion current and corrosion rate of epoxy-coated stainless steel and after nanocoating with decahydrobenzo[8]annulene-5,10-disemicarbazone and TiN were calculated by equation $\Delta E/\Delta I = \beta_a \beta_c / 2.303 I_{corr} (\beta_a + \beta_c)$ and $C. R (mmpy) = 0.1288 I_{corr} (mA/cm^2) \times Eq. Wt (g) / \rho (g/cm^3)$ and their values were mentioned in table4.5.3. The results of table3 and figure7 confirmed that

epoxy-coated stainless steel exhibited more electrode potential and corrosion current when coated with decahydrobenzo[8] annulene-5,10-disemicarbazone and TiN their values were decreased. It was also observed that anodic current increased with epoxy-coated stainless steel whereas cathodic current decreased but nanocoating and filler compounds reduced anodic current and enhanced cathodic current. Potentiostat results show that nanocoating and filler compounds minimized corrosion rate and increased surface coverage area and coating efficiency

Table3 Potentiostat of nanocoating decahydrobenzo[8]annulene-5,10-disemicarbazone and TiN filler for epoxycoated stainless steel

NC	ΔE (mV)	ΔI	β_a	β_c	I_{corr} (mA/cm ²)	K (mmpy)	?	%CE	C (mM)
NC(0)	-704	187	295	197	13.64	417	0	0	0.0
NC(4)	-251	24	35	315	1.31	39	0.91	91	50
NC(TiN)	-244	21	31	320	1.05	31	0.93	93	20



Conclusion

Nanocoating compound decahydrobenzo[8]annulene-5,10-disemicarbazone and TiN filler were formed composite barrier on the surface of epoxy-coated stainless steel. The results of thermal parameters and coating efficiencies were indicated that composite barrier is stable in corrosive environment. All scientific observations indicate that these nanocoating and filler compounds mitigate corrosion rate. The values of thermal parameters show that they form stable barrier on the surface of base material. It is noticed that these compounds accommodate more surface coverage areas. Composite barrier stops osmosis or diffusion process of pollutants. Nanocoating and filler compounds improve the life of base material and durability.

Acknowledgement

Author is thankful to The UGC-New for providing financial grant for this work. Author holds deep sense of gratitude for Professor Sanjoy Misra. Author is grateful to Professor G Udhaybhanu, IITDhanbad who provided laboratory facilities.

References

- Bhadra S, Singh N K and Khastgir D (2011), Polyaniline based anticorrosive and anti-molding coating, *Journal of Chemical Engineering and Materials Science* Vol.2(1) 1-11.
- Szabo T, Molnar-Nagy L, and Telegdi J (2011), Self-healing microcapsules and slow release microspheres in paints, *Progress in Organic Coatings*, 72, 52-57.
- Wen N T, Lin C S, Bai C Y, and Ger M D (2008) Structures and characteristics of Cr (III) based conversion coatings on electrogalvanized steels, *Surf. Coat. Technol.*, 203, 317.
- Boerio F J, Shah P (2005), Adhesion of injection molded PVC to steel substrates, *J of Adhesion* 81(6) 645-675.
- Deveci H, Ahmetti G and Ersoz M, (2012), Modified styrenes: Corrosion physico-mechanical and thermal properties evaluation, *Prog. Org. Coat.* 73 1-7.
- Genzer J (2005), Templating Surfaces with Gradient Assemblies, *J of Adhesion* 81 417-435.
- Leon-Silva U, Nicho M E (2010), Poly(3-octylthiophene) and polystyrene blends thermally treated as coating for corrosion protection of stainless steel 304, *J. Solid State Electrochem.*, 14 1487-1497.

- Baier R E (2006) Surface behaviour of biomaterials: Surface for biocompatibility, *J. Mater. Sci. Mater. Med.* 17 1057-1062.
- Rao BVA, Iqbal M Y and Sreehar B (2010), Electrochemical and surface analytical studies of the self assembled monolayer of 5-methoxy-2-(octadecylthiol) benzimidazole in corrosion protection of copper, *Electrochim. Acta*, 55 620-631.
- Liu X Y, Ma H Y and Hou M Z (2009), Self-assembled monolayers of stearic imidazoline on copper electrodes detected using electro chemical measurement, XPS, molecular simulation and FTIR, *Chinese Sci. Bull.* 54 374-381.
- Liao Q Q, Yue Z W and Zhou Q (2009), Corrosion inhibition effect of self-assembled monolayers of ammonium pyrrolidine dithiocarbamate on copper, *Acta Phys. Chin. Sin.* 25 1655-1661.
- Zhang D Q, He X M and Kim G S (2009), Arginine selfassembled monolayers against copper corrosion and synergistic effect of iodide ion, *J. Appl. Electrochem* 39 1193-1198.
- Sahoo R R and Biswas S K (2009), Frictional response of fatty acids on steel, *J. Colloid Interf. Sci.* 333 707-718.
- Raman R and Gawalt E S (2007), Selfassembled monolayers of alkanolic acid on the native oxide surface of SS316L by solution deposition, *Langmuir*, 23 2284-2288.
- Li D G, Chen S H and Zhao S Y (2006), The corrosion Inhibition of the self-assembled Au and Ag nanoparticles films on the surface of copper, *Colloid. Surface. A* 273 16-23.
- Cristiani P, Perboni G and Debenedetti A (2008), Effect of chlorination on the corrosion of Cu/Ni 70/30 condenser tubing, *Electrochim. Acta* 54 100-107.
- Cristiani P (2005), Solutions fouling in power station condensers, *Appl. Therm. Eng.* 25 2630-2640.
- Videla H and L K Herrera (2009), Understanding microbial inhibition of corrosion, *Electrochem Acta*, 39 229-234.
- Bibber J W (2009), Chromium free conversion coating for zinc and its alloys, *Journal of Applied Surface Finishing*, Vol. 2(4) 273-275.
- Ghareba G S and Omanovic S (2010), Interaction of 12-aminododecanoic acid with a carbon steel surface: Towards the development of 'green' corrosion inhibitors, *Corrosion Sci.* 52 2104-2113.